

Observation of TeV gamma ray extended sources with ARGO-YBJ

S. VERNETTO^{1,2}, S.Z. CHEN³ AND G. DI SCIASCIO⁴ FOR THE ARGO-YBJ COLLABORATION.

¹ *INAF, Osservatorio Astrofisico di Torino, Italy*

² *INFN, Sezione di Torino, Italy*

³ *Particle & Astrophysics Center, IHEP, CAS, Beijing, P.R.China*

⁴ *INFN, Sezione di Roma Tor Vergata, Viale della Ricerca Scientifica 1, Roma, Italy*

vernetto@to.infn.it

Abstract: A large fraction of unidentified TeV gamma-ray sources observed in the Galaxy are spatially extended raising the question of why there are so few point-like VHE sources. The study of these objects is important because the extended emission could be the result of cosmic ray interactions with the ambient medium which provides the target to produce TeV gamma-rays. The instrument sensitivity decreases for extended sources, however the shower detectors, with large fields of view, are less affected with respect to Cerenkov telescopes. The ARGO-YBJ experiment (Yangbajing Cosmic Ray Laboratory, Tibet, China, 4300 m asl) is an air shower detector able to observe VHE gamma rays at energies above a few hundred GeV with an integrated sensitivity ranging from 0.24 to ~ 1 Crab units, depending on the declination. In this paper the observation of galactic extended sources with ARGO-YBJ during 5 years is reviewed.

Keywords: ARGO-YBJ, Gamma Ray Astronomy, Extended Sources, Extensive Air Showers.

1 Introduction

The study of TeV γ -ray extended sources has been recognized as an important tool to investigate the sources of cosmic rays. Some authors suggest that the observed degree-scale extended emission could be produced by high-energy cosmic rays escaping from the source and diffusing in the interstellar medium (ISM) [1]. The γ -ray emission should result from the interaction of these cosmic rays with the ISM particles. Such extended emission regions should be visible as VHE γ -ray sources with fluxes of order 10^{-11} erg cm⁻² s⁻¹ above 100 GeV. Recently, Giacinti et al. [2] found that the diffusion of cosmic rays and electrons around point sources is strongly anisotropic and shows filamentary structures.

Ground based gamma ray detectors, both air shower arrays and Cherenkov telescopes, lose sensitivity observing extended sources. Air shower arrays, however, due to the large field of view (FOV) are less affected than Cherenkov instruments.

The ARGO-YBJ experiment, located at the YangBaJing Cosmic Ray Laboratory (Tibet, P.R. China, 4300 m a.s.l., 606 g/cm²), is a full coverage air shower array able to detect the cosmic radiation with an energy threshold of a few hundred GeV. It consists of a $\sim 74 \times 78$ m² carpet made of a single layer of Resistive Plate Chambers (RPCs) with $\sim 92\%$ of active area, surrounded by a partially instrumented ($\sim 20\%$) area up to $\sim 100 \times 110$ m². The apparatus is made of 18360 “pads” of size 55.6 \times 61.8 cm² which are the space-time “pixels” of the detector. The showers firing a number of pads $N_{pad} \geq 20$ in the central carpet generate the trigger.

ARGO-YBJ started collecting data in July 2006 with the central carpet, and the full apparatus was in operation from November 2007 to January 2013, with a duty cycle $> 86\%$. The trigger rate is ~ 3.5 kHz with a dead time of 4%. The detector characteristics are described in [3, 4, 5].

The detector performance (angular resolution, pointing accuracy, energy scale calibration) and the operation sta-

bility are monitored on a monthly basis by observing the Moon shadow, i.e., the deficit of CR detected in the Moon direction [6]. Details on the analysis procedure for gamma ray astronomy (e.g., reconstruction algorithms, data selection, background evaluation, systematic errors) are discussed in [7, 8, 9, 10, 11, 12].

In this paper the observation of 3 galactic TeV γ -ray extended sources in the northern hemisphere by ARGO-YBJ are reviewed.

2 MGRO J1908+06

The extended gamma ray source MGRO J1908+06 was discovered in 2007 by Milagro in a survey of the Galactic plane at a median energy of ~ 20 TeV [13]. The source was later observed by HESS. [14] and VERITAS [15]. The proximity of MGRO J1908+06 to the *Fermi* LAT pulsar PSR J1907+0602 suggested to identify it with the wind nebula of the pulsar [16, 18].

Fig. 1 shows the significance map obtained by ARGO-YBJ in ~ 3 years, using the events with a number of fired pads $N_{pad} \geq 60$. The source signal reaches 6.2 standard deviations (s.d.).

To evaluate the position and extension of the source, we assume a shape described by a symmetrical two-dimensional Gaussian function with r.m.s. σ_{ext} . We found the best-fit position at R.A. = $19^h 08^m 1^s$ and decl. = $6^\circ 24'$, with a statistical error of $12'$ and a systematic error of $6'$ per axis. The position found is consistent with the Milagro and HESS measurements. The value of the extension σ_{ext} that best fits the data is $0.49^\circ \pm 0.22^\circ$, and is consistent with the H.E.S.S. estimation of 0.34° .

The energy spectrum obtained in the energy range 1-20 TeV is: $dN/dE = 6.1 \pm 1.4 \times 10^{-13} (E/4 \text{ TeV})^{-2.54 \pm 0.36}$ photons cm⁻² s⁻¹ TeV⁻¹, shown in Fig. 2 together with those reported by other detectors [13, 14, 16, 19]. This spectrum is consistent with the Milagro results, but not with the HESS best fit in the 1-10 TeV energy range, where

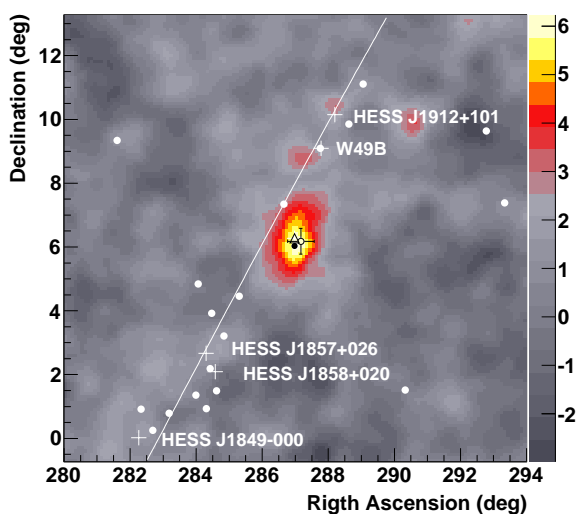


Figure 1: ARGO-YBJ significance map of the MGRO J1908+06 region. Open circle: position of the center of MGRO J1908+06, as measured by Milagro. The error bars give the linear sum of the statistical and systematic errors. Open triangle: centroid of HESS J1908+063. Black filled circle: Fermi pulsar PSR J1907+0602. White filled circles: Fermi gamma ray sources, from the 2nd Fermi-LAT Catalogue [20]. White crosses: TeV sources detected by HESS. The white line represents the Galactic plane.

the flux measured by ARGO-YBJ at 4 TeV is a factor of 2.6 larger. At ~ 20 TeV the ARGO-YBJ, HESS and Milagro fluxes are consistent within the errors, and are also in agreement with the first Milagro measurement [13].

Since the diffuse Galactic emission could contribute to the observed signal, an accurate evaluation of this contamination was performed analyzing the data of two sky regions located at both sides of the source and centered at the same galactic latitude. According to our estimate, the Galactic diffuse emission accounts for $33 \pm 18\%$ using events with a number of fired pads $N_{pad} = 20 - 59$, and for $\leq 15\%$ using events with a higher N_{pad} . The contribution is larger for small events because of the broader PSF and because the diffuse spectrum is steeper than the source spectrum. To avoid this contamination, only events with $N_{pad} \geq 60$ have been used to evaluate the extension and the spectrum of MGRO J1908+06.

For a complete description of the analysis and results, see [9], and for a new possible interpretation of the extended emission region, see [17].

3 HESS J1841-055

HESS J1841-055 is an unidentified VHE gamma-ray source discovered by the HESS collaboration during the Galactic plane survey [21]. Its image shows a high extension, the measured axes for an elongated two-dimensional Gaussian shape being $0^\circ.41 \pm 0^\circ.04$ (major) and $0^\circ.25 \pm 0^\circ.02$ (minor). HESS J1841-055, therefore, is one of the most extended sources in the VHE γ -ray band. The spectrum is best fitted by a simple power law with photon index $\alpha = -2.41 \pm 0.08$ in the energy range 0.54 TeV to 80 TeV. The integral flux is 9.1×10^{-12} photons $\text{cm}^{-2} \text{s}^{-1}$ at energies above 1 TeV, about 0.40 Crab units.

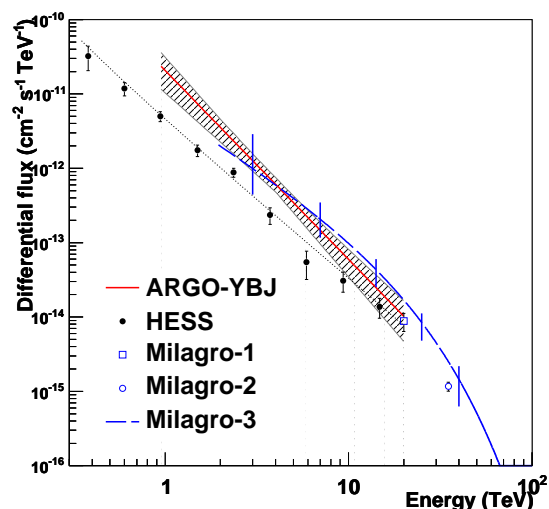


Figure 2: Gamma ray flux from MGRO J1908+06 measured by ARGO-YBJ and other detectors. The dashed area indicates 1 s.d. error.

To date, no obvious counterpart has been found at other wavelengths. The wide VHE γ -ray morphology suggests that HESS J1841-055 may be the blend of multiple sources. Aharonian et al. [21] found four candidates which could be responsible for at least part of the entire VHE γ -ray emission: the two pulsars PSR J1841-0524 and PSR J1838-0549, the diffuse source G26.6-0.1, which is a candidate SNR based on its ASCA spectrum, and finally, the high-mass XB AX J1841.0-0536.

The significance map around HESS J1841-055, as observed by ARGO-YBJ using events with $N_{pad} > 60$, is shown in Fig. 3.

The highest significance is 5.3 s.d. at $\alpha = 18^h 39^m$ and $\delta = 6^\circ 3'$ (J2000), which is displaced 0.7° from the center of HESS J1841-055. However, most of the excess overlaps the extended region of HESS J1841-055 and its gravity center ($\alpha = 18^h 40^m \pm 12^m$ and $\delta = -5^\circ 52' \pm 13'$), obtained using all the pixels with significance greater than 3 s.d. within $3^\circ \times 3^\circ$ around HESSJ1841-055, is 0.4° off the center of HESS J1841-055. These displacements may be caused by different concurring effects beside fluctuation. (1) Complex morphology. According to the HESS result, HESS J1841-055 possibly has two or three peaks and the positions of the two largest ones are both 0.44° off the center. (2) The systematic pointing error of ARGO-YBJ is 0.2° , slightly increasing at the boundary of the ARGO-YBJ FOV. (3) The contribution of the nearby VHE source HESS J1837-069, whose flux is 17% the Crab Nebula flux at energies > 1 TeV, according to HESS [22].

The intrinsic extension of HESS J1841-055 is determined by fitting the angular distribution of the events exceeding the background. To achieve a good angular resolution, only events with $N_{pad} > 100$ are used in this fit. Assuming a spectral index -2.3 , the intrinsic extension is determined to be $\sigma_{ext} = (0.40^{+0.32}_{-0.22})^\circ$. This result is consistent with the estimation by the HESS collaboration [21].

Assuming an intrinsic extension $\sigma_{ext} = 0.40^\circ$, we estimate the spectrum of HESS J1841-055. The differential flux in the energy range 0.9 - 50 TeV is $dN/dE = (9.0 \pm 1.6) \times 10^{-13} (E/5 \text{ TeV})^{-2.32 \pm 0.23}$ photons $\text{cm}^{-2} \text{s}^{-1} \text{TeV}^{-1}$ (see

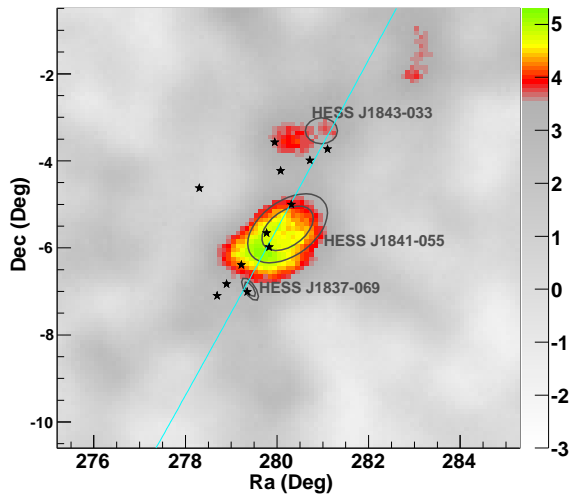


Figure 3: The significance map around HESS J1841-055 as observed by ARGO-YBJ. The two ellipses for HESS J1841-055 and HESS J1837-069 indicate their positions and the 68% and 90% contours of their extension regions, according to HESS [21]. The position and possible extension of HESS J1843-33 are marked with ellipse [24]. The stars mark the location of the GeV γ -ray sources around HESS J1841-055 in the second Fermi-LAT catalog [20]. The solid line indicates the Galactic plane.

Fig. 4). At 5 TeV the flux is 3.5 times larger than the flux determined by the HESS. According to our estimates, the diffuse emission from the Galactic plane contributes to the measured flux of HESS J1841-055 for less than 4%, and should not account for the observed discrepancy.

A detailed presentation of the results of ARGO-YBJ concerning this source are given in [12].

4 MGRO 2031+41 and the Cygnus X region

The Cygnus X region is one of the most luminous region of the northern gamma ray sky and it is rich in potential cosmic ray accelerator sites, e.g. Wolf Rayet stars, OB associations and SN remnants. Several VHE gamma ray sources have been detected, the brightest ones being the extended sources MGRO J2019+37 and MGRO J2031+41/TEV J2032+4130, whose locations are consistent with two *Fermi* pulsars. Moreover, in a position consistent MGRO J2031+41, *Fermi* detected a complex extended source, attributed to the emission of freshly accelerated cosmic rays interacting with gas and radiation, filling a bubble (a “cocoon”) carved by stellar winds and multiple supernovae shock waves [25].

The significance map of this region obtained by ARGO-YBJ is shown in Fig. 5. A signal of significance larger than 6 standard deviations is present at the position of MGRO J2031+41. The energy spectrum measured by ARGO-YBJ is $dN/dE = 1.40 \pm 0.34 \times 10^{-11} (E/1 \text{ TeV})^{-2.83 \pm 0.37}$ photons $\text{cm}^{-2} \text{ s}^{-1} \text{ TeV}^{-1}$, in the energy range 0.6-7 TeV.

The integral flux is 31% that of the Crab Nebula at energies above 1 TeV, higher than the flux determined by the HEGRA [26] and MAGIC [27] experiments (5% and 3% Crab units, respectively), while is in good agreement with

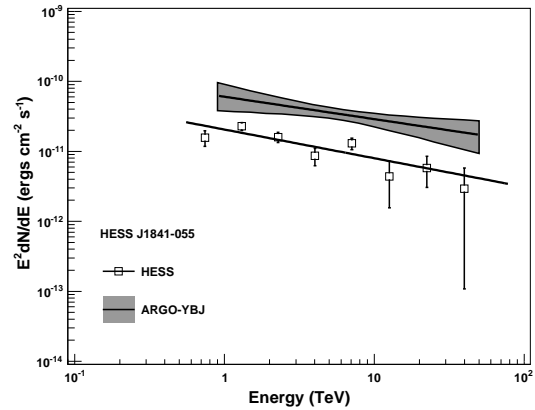


Figure 4: Energy density spectrum of HESS J1841-055 as measured by the ARGO-YBJ and HESS experiments. The shaded area indicates the 1 s.d. error band for the ARGO-YBJ data.

the Milagro result [28, 29] (see Fig. 6). For this source the expected contribution from the Galactic diffuse emission is $\sim 10\%$.

Concerning the source MGRO J2019+37, which is the Milagro’s most significant detection after the Crab Nebula at energies of ~ 20 TeV, the ARGO-YBJ map does not show any excess. The obtained 90%CL upper limits do not conflict with the Milagro result [29]. On the other hand, in a scanning of the Cygnus region, VERITAS detected a faint extended complex of sources at the MGRO J2019+37 position, with a total flux of the order of 1% Crab Units [30]. The possible variability of one of these sources could explain the disagreement. As a matter of fact, the Milagro observations do not overlap in time the ARGO-YBJ and VERITAS ones. A detailed description of the ARGO-YBJ results about the Cygnus region are given in [10].

5 Discussion and conclusions

Since November 2007 to January 2013 the ARGO-YBJ experiment monitored with high duty cycle the northern sky at TeV photon energies [31].

Emission from 3 extended sources (MGRO 1908+06, MGRO 2031+41 and HESS 1841-055) has been observed with high statistical significance. The obtained energy spectra are in disagreement with IACT results being the measured fluxes higher by a factor ranging from ~ 3 (for MGRO J1908+06 and HESS J1841-055) to ~ 10 (for MGRO J2031+41).

The origin of such a discrepancy is not clear. Since no disagreement exists for the flux measured from the Crab Nebula [32], the problem seems to be related to the source extension. Some systematic effect and/or an incorrect evaluation of the background by some of the experiments could be the cause.

Concerning ARGO-YBJ, the source extension should not introduce any further systematic with respect to a point source. The large FOV ensures that no events are loss, and the analysis procedure is exactly the same for extended and point sources. The possible causes of systematic errors listed below have been accurately evaluated and should not be responsible of such a large overestimation of the flux.

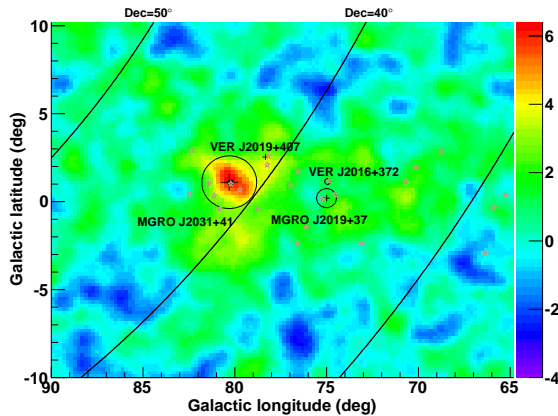


Figure 5: Significance map of the Cygnus region. The position of 4 known VHE gamma ray sources are also reported.

1) Background evaluation. The cosmic ray background evaluation is performed using two different techniques, the “time swapping method” [33] and the “direct integral method” [34], that give fully consistent results. They are based on the assumption that the shape of the distribution of cosmic rays in local coordinates is constant in a time interval $\Delta T \sim 3$ hours. For any bin of the sky maps, the events with the same declination recorded in ΔT are used to evaluate the corresponding background. The possible presence of other sources at the same declination and with a difference in right ascension less than $15^\circ \times \Delta T$ could artificially increase the background by a small amount, and consequently decrease the possible source signal.

The anisotropy of cosmic ray could also introduce a systematics in some regions of the sky, that is corrected with the normalization procedure described in [8].

However, if an erroneous estimation of the background was done, the significance maps would present a systematic excess or deficit over a large area. Let’s consider the map of Fig.1. The measured flux of MGRO J1908+06 is 2.6 times larger than the one obtained by H.E.S.S. A background underestimation able to produce such a larger flux, would produce also an excess of ~ 4 standard deviations over all the map. On the contrary, excluding the MGRO J1908+06 contribution, the distribution of the excess significances of the map is a Gaussian distribution centered at zero and with r.m.s. consistent with unity. The background evaluation can be checked directly by the distribution of the map excesses.

2) A pointing error (periodically checked with the position of the Moon Shadow [6]), would cause a loss of signal instead of an overestimation.

3) The error on the energy scale, also checked with the Moon Shadow, is found to be less than 13% [6] and cannot produce such a large discrepancy among the fluxes.

4) The diffuse emission from the Galactic Plane in the source region could increase the signal. However, according to our evaluation, its contribution to the flux of the three observed sources should be less than 4-15%.

In conclusion, we do not find in our data a possible systematics that could justify the observed large fluxes. The overall systematics should lead to at most a 30% error on the flux.

On the other hand, Cherenkov telescopes, due to their limited FOV, might count the extended gamma ray emis-

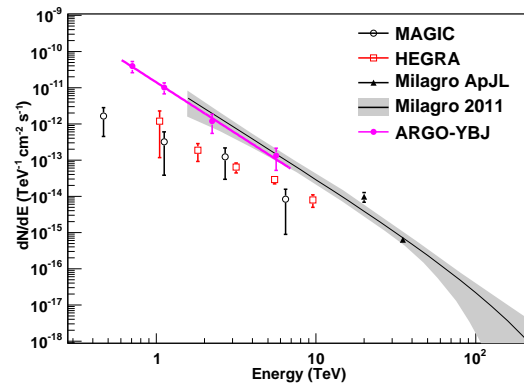


Figure 6: Spectrum of MGRO J2031+41 measured by ARGO-YBJ and other detectors.

sion as background, especially when using the “wobble” mode, and consequently underestimate the source signal. A joint comparison of air shower detectors and Cherenkov telescopes techniques would be useful to find the origin of the discrepancy.

References

- [1] A. Neronov, & D. Semikoz, Phys. Rev. D 85 (2012) 083008.
- [2] G. Giacinti et al., Phys. Rev. Lett. 108 (2012) 261101.
- [3] C. Bacci et al., NIM A 443 (2000) 342.
- [4] G. Aielli et al., NIM A 562 (2006) 92.
- [5] G. Aielli et al., NIM A 608 (2009) 246.
- [6] B. Bartoli et al., Phys. Rev. D 84 (2011) 022003.
- [7] G. Aielli et al. ApJL 714 (2010) 208.
- [8] B. Bartoli et al. ApJ 734 (2011) 110.
- [9] B. Bartoli et al. ApJ 760 (2012) 110.
- [10] B. Bartoli et al., ApJL 745 (2012) 22.
- [11] B. Bartoli et al., ApJ 758 (2012) 2.
- [12] B. Bartoli et al., ApJ 767 (2013) 99.
- [13] A.A. Abdo et al., ApJL 664 (2007) L91.
- [14] F. Aharonian et al., A&A 499 (2009) 723.
- [15] Ward, J.E., et al., AIP Conf. Proc. 1085 (2008) 301.
- [16] A.A. Abdo et al., ApJL 700 (2009) L27.
- [17] S.Z. Chen et al., these proceedings (2013).
- [18] A.A. Abdo et al., ApJ 711 (2010) 64.
- [19] A.J. Smith et al. Proc. Fermi Symposium, Washington, D.C., 2009 Nov. 2-5 (arXiv:1001.3695).
- [20] P.L. Nolan et al., ApJ Suppl. 199 (2012) 31.
- [21] F. Aharonian et al., A&A 477 (2008) 353.
- [22] F. Aharonian et al., ApJ 636 (2006) 777.
- [23] A.A. Abdo et al. ApJ 753 (2012) 159.
- [24] S. Hoppe, in Proc. 30th ICRC (2007) 579.
- [25] M. Ackermann et al., Science 334 (2011) 1103.
- [26] F. Aharonian et al., A&A 431 (2005) 197.
- [27] J. Albert et al., ApJ, 675 (2008) L25.
- [28] E. Bonamente, J. Galbraith-Frew & P. Huntemeyer, Proc. 32nd ICRC, 7 (2011) 7.
- [29] A.A. Abdo et al. ApJ 753 (2012) 159.
- [30] E. Aliu et al., Proc. 32nd ICRC, 7 (2011) 228.
- [31] S.Z. Chen et al., Proc 33nd ICRC (2013).
- [32] S. Vernetto et al., these proceedings (2013).
- [33] D.R. Alexandreas et al., NIM A328 (1993) 570.
- [34] R. Fleishner et al., ApJ 603 (2004) 355.